

Constraints on new physics from the quark mixing unitarity triangle

(UTfit Collaboration)

M. Bona,¹ M. Ciuchini,² E. Franco,³ V. Lubicz,² G. Martinelli,³ F. Parodi,⁴

M. Pierini,⁵ P. Roudeau,⁶ C. Schiavi,⁴ L. Silvestrini,³ A. Stocchi,⁶ and V. Vagnoni⁷

¹Laboratoire d'Annecy-le-Vieux de Physique des Particules LAPP, IN2P3/CNRS, Université de Savoie

²Dip. di Fisica, Università di Roma Tre and INFN, Sez. di Roma Tre, I-00146 Roma, Italy

³Dip. di Fisica, Università di Roma "La Sapienza" and INFN, Sez. di Roma, I-00185 Roma, Italy

⁴Dip. di Fisica, Università di Genova and INFN, I-16146 Genova, Italy

⁵Department of Physics, University of Wisconsin, Madison, WI 53706, USA

⁶Laboratoire de l'Accélérateur Linéaire, IN2P3-CNRS et Université de Paris-Sud, BP 34, F-91898 Orsay Cedex, France

⁷INFN, Sez. di Bologna, I-40126 Bologna, Italy

The status of the Unitarity Triangle beyond the Standard Model including the most recent results on Δm_s , on dilepton asymmetries and on width differences is presented. Even allowing for general New Physics loop contributions the Unitarity Triangle must be very close to the Standard Model result. With the new measurements from the Tevatron, we obtain for the first time a significant constraint on New Physics in the B_s sector. We present the allowed ranges of New Physics contributions to $\Delta F = 2$ processes, and of the time-dependent CP asymmetry in $B_s \rightarrow J/\Psi\phi$ decays.

In the last decade, flavour physics has witnessed unprecedented experimental and theoretical progress, opening the era of precision flavour tests of the Standard Model (SM). The advent of B factories, with the measurements of the angles of the Unitarity Triangle (UT), has opened up the possibility of the simultaneous determination of SM and New Physics (NP) parameters in the flavour sector. As shown below, with the most recent improvements obtained at the B factories and at the Tevatron, the UT analysis in the presence of NP has reached an accuracy comparable to the SM analysis, providing at the same time very stringent constraints on NP contributions to $\Delta F = 2$ processes.

While in general all the constraints have been improved, three remarkable results have boosted the precision of the UT analysis beyond the SM. First, the CDF collaboration presented the first measurement of $B_s - \bar{B}_s$ mass difference Δm_s [1], which reduces the uncertainty of the SM fit [2] and has a strong impact on the determination of the Universal Unitarity Triangle (UUT) [3] in models with Minimal Flavour Violation (MFV) [4, 5]. Moreover, it allows for the first time to put a bound on the absolute value of the amplitude for B_s oscillations [6]. Second, the measurement of the dimuon asymmetry in $p\bar{p}$ collisions by the D0 experiment [7] can be translated into a bound on the phase of the same amplitude [8]. Third, the measurements of the width difference for B_q mesons provide another constraint on the phase of the mixing amplitudes, complementary to the one given by dilepton asymmetries [9].

In this Letter, we first discuss extensions of the SM with MFV, in which no new source of flavour and CP violation is present beyond the SM Yukawa couplings. We analyze the impact of Δm_s on the UUT determination, where the ratio $\Delta m_d/\Delta m_s$ plays a crucial role since it is independent of NP contributions. We find that the UUT analysis has now an accuracy very close to the

SM UT fit. Using instead the information coming from the individual measurements of Δm_s , Δm_d and ε_K , we constrain NP contributions to the $\Delta F = 2$ Hamiltonian, both in the small and large $\tan\beta$ regimes. We find improved constraints on the NP scale Λ that suppresses non-renormalizable effective interactions.

We then turn to the most general case in which NP contributions with an arbitrary phase are allowed in all sectors, and obtain a fully model-independent determination of the CKM parameters $\bar{\rho}$ and $\bar{\eta}$. We simultaneously obtain the allowed range for the $\Delta F = 2$ amplitudes which can be used to test any extension of the SM, and the prediction for the time-dependent CP asymmetry $S_{J/\Psi\phi}$. For all our analyses we use the method described in refs. [10, 11] and the input values listed in ref. [12].

In the context of MFV extensions of the SM, it is possible to determine the parameters of the CKM matrix independently of the presence of NP, using the UUT construction, which is independent of NP contributions. In particular, all the constraints from tree-level processes and from the angle measurements are valid and the NP contribution cancels out in the $\Delta m_d/\Delta m_s$ ratio; the only NP dependent quantities are ε_K and (individually) Δm_d and Δm_s , because of the shifts δS_0^K and δS_0^B of the Inami-Lim functions in $K - \bar{K}$ and $B_{d,s} - \bar{B}_{d,s}$ mixing processes. With only one Higgs doublet or at small $\tan\beta$, these two contributions are dominated by the Yukawa coupling of the top quark and are forced to be equal. For large $\tan\beta$, the additional contribution from the bottom Yukawa coupling cannot be neglected and the two quantities are in general different. In both cases, one can use the output of the UUT given in Tab. I and in the left plot of Fig. 1 to obtain a constraint on $\delta S_0^{K,B}$ using ε_K and Δm_d . We get $\delta S_0 = \delta S_0^K = \delta S_0^B = -0.12 \pm 0.32$ for small $\tan\beta$, while for large $\tan\beta$ we obtain $\delta S_0^B = 0.26 \pm 0.72$ and $\delta S_0^K = -0.18 \pm 0.38$. Using the procedure detailed in [5], these bounds can be translated into lower bounds

on the MFV scale Λ :

$$\begin{aligned}\Lambda &> 5.9 \text{ TeV @95\% Prob. for small } \tan\beta \\ \Lambda &> 5.4 \text{ TeV @95\% Prob. for large } \tan\beta\end{aligned}\quad (1)$$

significantly stronger than our previous results $\Lambda > 3.6$ TeV and $\Lambda > 3.2$ TeV for small and large $\tan\beta$ respectively [11].

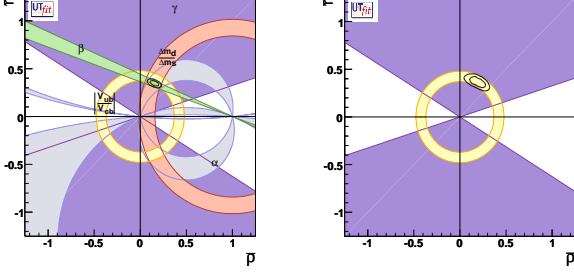


FIG. 1: Determination of $\bar{\rho}$ and $\bar{\eta}$ from the constraints on α , β , γ , $|V_{ub}/V_{cb}|$, $\Delta m_d/\Delta m_s$ (UUT fit, left) and from the constraints on α , β , γ , $|V_{ub}/V_{cb}|$, Δm_d , Δm_s , ϵ_K , A_{SL} , A_{CH} and $\Delta\Gamma_q/\Gamma_q$ (generalized NP fit, right). In the right plot, only tree-level constraints are shown.

Parameter	Output	Parameter	Output
$\bar{\rho}$	0.154 ± 0.032	$\bar{\eta}$	0.347 ± 0.018
$\alpha[^\circ]$	91 ± 5	$\beta[^\circ]$	22.2 ± 0.9
$\gamma[^\circ]$	66 ± 5	$\sin 2\beta_s$	0.037 ± 0.002
$\sin 2\beta$	0.704 ± 0.023	$\text{Im}\lambda_t [10^{-5}]$	14.0 ± 0.8
$V_{ub}[10^{-3}]$	3.69 ± 0.15	$V_{cb}[10^{-2}]$	4.18 ± 0.07
$V_{td}[10^{-3}]$	8.6 ± 0.3	$ V_{td}/V_{ts} $	0.210 ± 0.008
R_b	0.381 ± 0.015	R_t	0.915 ± 0.033

TABLE I: Determination of UUT parameters from the constraints on α , β , γ , $|V_{ub}/V_{cb}|$, and $\Delta m_d/\Delta m_s$ (UUT fit).

We now turn to the UT analysis in the presence of arbitrary NP. Following ref. [11], we incorporate general NP loop contributions in the fit in a model independent way, parametrizing the shift induced in the $B_q-\bar{B}_q$ mixing frequency (phase) with a parameter C_{B_q} (ϕ_{B_q}) having expectation value of one (zero) in the SM [13]:

$$C_{B_q} e^{2i\phi_{B_q}} = \frac{\langle B_q | H_{\text{eff}}^{\text{full}} | \bar{B}_q \rangle}{\langle B_q | H_{\text{eff}}^{\text{SM}} | \bar{B}_q \rangle} = 1 + \frac{A_q^{\text{NP}}}{A_q^{\text{SM}}} e^{2i\phi_q^{\text{NP}}}\quad (2)$$

with $q = d, s$, plus an additional parameter $C_{\varepsilon_K} = \text{Im}\langle K^0 | H_{\text{eff}}^{\text{full}} | \bar{K}^0 \rangle / \text{Im}\langle K^0 | H_{\text{eff}}^{\text{SM}} | \bar{K}^0 \rangle$. As shown in refs. [11, 14], the measurements of UT angles strongly reduced the allowed parameter space in the B_d sector. On the other hand, in previous analyses the B_s sector was completely untested in the absence of stringent experimental constraints. Recent experimental developments

allow to improve the bounds on NP in several ways. First, the measurement of Δm_s [1] and of $\Delta\Gamma_s$ [15] provide the first constraints on the ϕ_{B_s} vs. C_{B_s} plane. Second, the improved measurement of A_{SL} in B_d decays [16] and the recently measured CP asymmetry in dimuon events (A_{CH}) [7] further constrain the C_{B_q} and ϕ_{B_q} parameters. They also strongly disfavour the solution with $\bar{\rho}$ and $\bar{\eta}$ in the third quadrant, which now has only 1.0% probability. Finally, $\Delta\Gamma_d$ [17] helps in reducing further the uncertainty in C_{B_d} .

The use of A_{CH} and $\Delta\Gamma_q$ to bound C_{B_q} and ϕ_{B_q} deserve some explanation, while for all the other constraints we refer the reader to ref. [11]. The dimuon charge asymmetry A_{CH} can be written as:

$$\frac{(\chi - \bar{\chi})(P_1 - P_3 + 0.3P'_8)}{\xi(P_1 + P_3) + (1 - \xi)P_2 + 0.28P_7 + 0.5P'_7 + 0.69P_{13}}$$

in the notation of ref. [7], where the definition and the measured values for the P parameters can be found. We have $\chi = f_d\chi_d + f_s\chi_s$, $\bar{\chi} = f_d\bar{\chi}_d + f_s\bar{\chi}_s$ and $\xi = \chi + \bar{\chi} - 2\chi\bar{\chi}$, where we have assumed equal semileptonic widths for B_s and B_d mesons, $f_d = 0.397 \pm 0.010$ and $f_s = 0.107 \pm 0.011$ are the production fractions of B_d and B_s mesons respectively [18] and χ_q and $\bar{\chi}_q$ are given by the expression

$$\chi_q^{(-)} = \frac{\frac{\Delta\Gamma_q^2}{\Gamma_q^2} + 4\frac{\Delta m_q^2}{\Gamma_q^2}}{\frac{\Delta\Gamma_q^2}{\Gamma_q^2}(z_q^{(-)} - 1) + 4(2z_q^{(-)} + \frac{\Delta m_q^2}{\Gamma_q^2}(1 + z_q^{(-)}))}\quad (3)$$

with $z_q = |q/p|_q^2$ and $\bar{z}_q = |p/q|_q^2$. Finally, using the results of [19] and following the notation of [11], we have

$$\frac{\Delta\Gamma_q}{\Delta m_q} = \text{Re } \mathcal{P}, \quad \left| \frac{q}{p} \right|_q - 1 = -\frac{1}{2} \text{Im } \mathcal{P}\quad (4)$$

where

$$\begin{aligned}\mathcal{P} = & -2\frac{\kappa}{C_{B_q}} \left\{ e^{2\phi_{B_q}} \left(n_1 + \frac{n_6 B_2 + n_{11}}{B_1} \right) \right. \\ & - \frac{e^{(\phi_q^{\text{SM}} + 2\phi_{B_q})}}{R_t^q} \left(n_2 + \frac{n_7 B_2 + n_{12}}{B_1} \right) + \frac{e^{2(\phi_q^{\text{SM}} + \phi_{B_q})}}{R_t^{q^2}} \\ & \left(n_3 + \frac{n_8 B_2 + n_{13}}{B_1} \right) + e^{(\phi_q^{\text{Pen}} + 2\phi_{B_q})} C_q^{\text{Pen}} \left(n_4 + n_9 \frac{B_2}{B_1} \right) \\ & \left. - e^{(\phi_q^{\text{SM}} + \phi_q^{\text{Pen}} + 2\phi_{B_q})} \frac{C_q^{\text{Pen}}}{R_t^q} \left(n_5 + n_{10} \frac{B_2}{B_1} \right) \right\}\end{aligned}\quad (5)$$

with $\kappa = -2\pi m_b^2 / (3M_W^2 \eta_B S_0(x_t))$, the B parameters and the magic numbers n_i given in ref. [11] ($SU(3)$ breaking effects in the magic numbers can be neglected given the present errors) and $R_t^q = |V_{tq} V_{tb}^*| / |V_{cq} V_{cb}^*|$. As discussed in ref. [11], C_q^{Pen} and ϕ_q^{Pen} parametrize possible NP contributions to $\Delta B = 1$ penguins. Concerning $\Delta\Gamma_s$, since the available experimental measurements are not directly sensitive to the phase of the mixing amplitude,

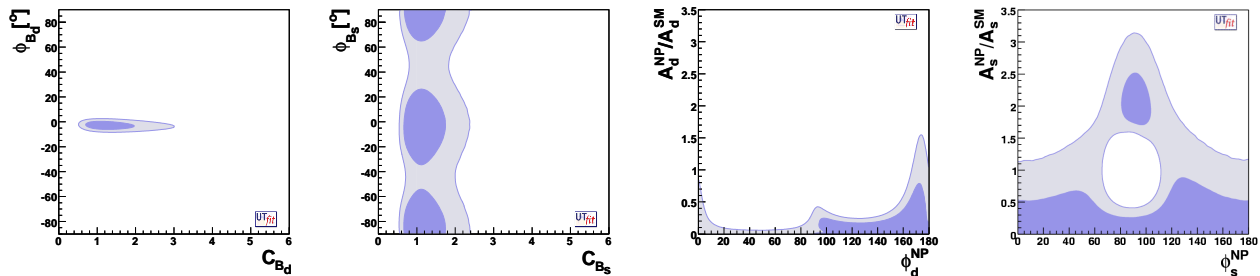


FIG. 2: From left to right, constraints on ϕ_{B_d} vs. C_{B_d} , ϕ_{B_s} vs. C_{B_s} , ϕ_d^{NP} vs. $A_d^{\text{NP}}/A_d^{\text{SM}}$ and ϕ_s^{NP} vs. $A_s^{\text{NP}}/A_s^{\text{SM}}$ from the NP generalized analysis.

they are actually a measurement of $\Delta\Gamma_s \cos 2(\phi_{B_s} - \beta_s)$ in the presence of NP [9]. To assess the constraining power of leptonic asymmetries and width differences, we compare the SM predictions and the experimental results with the predictions in the presence of NP, see Tab. II and Fig. 3. We see that NP can produce dilepton asym-

	SM	SM+NP	exp	ref
$10^3 A_{\text{SL}}$	-0.71 ± 0.12	see Fig. 3	-0.3 ± 5	[16]
$10^3 A_{\text{CH}}$	-0.23 ± 0.05	see Fig. 3	$-13 \pm 12 \pm 8$	[7]
$10^3 \Delta\Gamma_d/\Gamma_d$	3.3 ± 1.9	2.0 ± 1.8	9 ± 37	[17]
$\Delta\Gamma_s/\Gamma_s$	0.10 ± 0.06	0.00 ± 0.08	0.25 ± 0.09	[15]

TABLE II: Predictions for A_{SL} , A_{CH} and $\Delta\Gamma_q/\Gamma_q$ in the SM or in the presence of NP, obtained without including these observables in the fit.

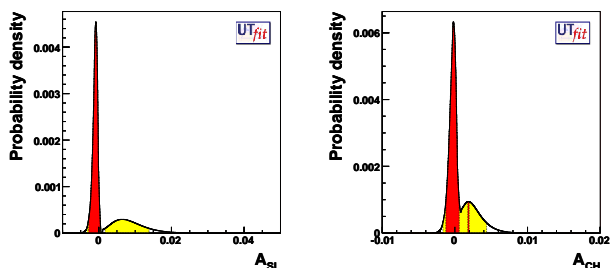


FIG. 3: Predictions for A_{SL} and A_{CH} in the presence of NP, obtained without including these observables in the fit. The lower peak in the p.d.f.'s correspond to values of ρ and η in the third quadrant.

metries ($\Delta\Gamma_s$) much larger (smaller) than the SM, so that including them in the fit improves the constraints on NP. For each value of (C_{B_q} , ϕ_{B_q}) we compute A_{SL} , A_{CH} and $\Delta\Gamma_s \cos 2(\phi_{B_s} - \beta_s)$ and use the experimental values to compute the weight of the given configuration. In ref. [8], the measurement of A_{CH} was used in a different way: A_{CH} was combined with the experimental value of

A_{SL} to obtain a value for A_{SL}^s . In principle, our method takes into account the correlations between the theoretical predictions for A_{SL} and A_{SL}^s . In addition, using A_{CH} instead of A_{SL}^s is more constraining since the theoretical range for A_{SL} is smaller than the present experimental error. In practice, however, these two effects are rather small.

The result of the fit is summarized in Tab. III. The bound on $\bar{\rho}$ and $\bar{\eta}$ is also shown in right plot of Fig. 1, while the bounds on the two ϕ_B vs. C_B planes are given in Fig. 2, together with the corresponding regions in the ϕ_q^{NP} vs. $A_q^{\text{NP}}/A_q^{\text{SM}}$ planes. The distributions for C_{B_q} , ϕ_{B_q} and C_{ε_K} are shown in Fig. 4. We see that the *non-standard* solution for the UT with its vertex in the third quadrant, which was present in the previous analysis [11], is now absent thanks to the improved value of A_{SL} by the BaBar Collaboration and to the measurement of A_{CH} by the D0 Collaboration (the lower peaks in Fig. 3 correspond to the *non-standard* solution and are now excluded). Furthermore, the measurement of Δm_s strongly constrains C_{B_s} , so that C_{B_s} is already known better than C_{B_d} . Finally, A_{CH} and $\Delta\Gamma_s$ provide stringent constraints on ϕ_{B_s} . Taking these constraints into account, we obtain

$$S_{J/\Psi\phi} = 0.09 \pm 0.60, \quad (6)$$

leaving open the possibility of observing large values of $S_{J/\Psi\phi}$ at LHCb. We point out an interesting correlation between the values of C_{B_d} and C_{B_s} that can be seen in Fig. 4. This completely general correlation is present since lattice QCD determines quite precisely the ratio ξ^2 of the matrix elements entering B_s and B_d mixing amplitudes respectively.

We conclude by noting that the fit produces a nonzero central value of ϕ_{B_d} . This is due to the difference in the SM fit between the angles measurement (in particular $\sin 2\beta$) and the sides measurement (in particular V_{ub} inclusive). More details on this difference can be found in ref. [2]. Further improvements in experimental data and in theoretical analyses are needed to tell whether this is just a fluctuation or we are really seeing a first hint of

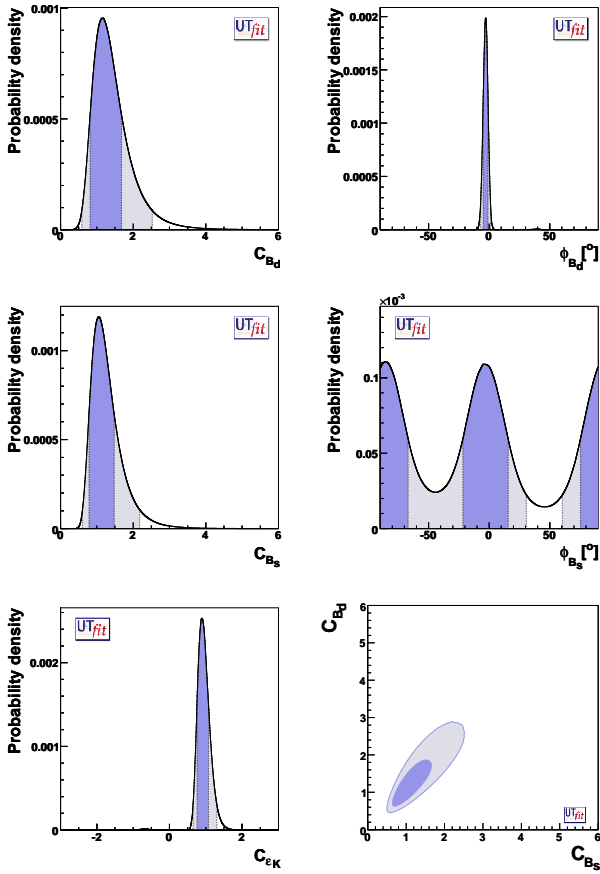


FIG. 4: Constraints on ϕ_{B_q} , C_{B_q} and C_{ε_K} coming from the NP generalized analysis. The correlation between C_{B_d} and C_{B_s} is also shown.

NP in the flavour sector.

We thank A.J. Buras, S. Giagu, A. Lenz, M. Rescigno and A. Weiler for useful discussions. This work has been supported in part by the EU network “The quest for unification” under the contract MRTN-CT-2004-503369.

[1] <http://www-cdf.fnal.gov/physics/new/bottom/060406.blessed-Bsmix/BsMixingMeasurement.pdf>
[2] M. Bona *et al.* [UTfit Collaboration], arXiv:hep-ph/0606167.
[3] A. J. Buras *et al.*, Phys. Lett. B **500**, 161 (2001).
[4] E. Gabrielli and G. F. Giudice, Nucl. Phys. B **433**, 3 (1995) [Erratum-ibid. B **507**, 549 (1997)]; M. Misiak, S. Pokorski and J. Rosiek, Adv. Ser. Direct. High Energy Phys. **15**, 795 (1998); M. Ciuchini, G. Degrossi, P. Gambino and G. F. Giudice, Nucl. Phys. B **534**, 3 (1998); C. Bobeth *et al.*, Nucl. Phys. B **726**, 252 (2005); M. Blanke, A. J. Buras, D. Guadagnoli and C. Tarantino, arXiv:hep-ph/0604057; G. Isidori and P. Paradisi, Phys. Lett. B **639**, 499 (2006).

Parameter	Output	Parameter	Output
C_{B_d}	1.25 ± 0.43	$\phi_{B_d} [^\circ]$	-2.9 ± 2.0
C_{B_s}	1.13 ± 0.35	$\phi_{B_s} [^\circ]$	$(-3 \pm 19) \cup (94 \pm 19)$
C_{ε_K}	0.92 ± 0.16		
$\bar{\rho}$	0.20 ± 0.06	$\bar{\eta}$	0.36 ± 0.04
$\alpha [^\circ]$	93 ± 9	$\beta [^\circ]$	24 ± 2
$\gamma [^\circ]$	62 ± 9	$\text{Im}\lambda_t [10^{-5}]$	14.6 ± 1.4
$V_{ub} [10^{-3}]$	4.01 ± 0.25	$V_{cb} [10^{-2}]$	4.15 ± 0.07
$V_{td} [10^{-3}]$	8.33 ± 0.61	$ V_{td}/V_{ts} $	0.203 ± 0.015
R_b	0.416 ± 0.027	R_t	0.887 ± 0.063
$\sin 2\beta$	0.748 ± 0.040	$\sin 2\beta_s$	0.039 ± 0.004

TABLE III: Determination of UT and NP parameters from the NP generalized fit.

[5] G. D’Ambrosio, G. F. Giudice, G. Isidori and A. Strumia, Nucl. Phys. B **645**, 155 (2002).
[6] M. Ciuchini and L. Silvestrini, Phys. Rev. Lett. **97**, 021803 (2006); Z. Ligeti, M. Papucci and G. Perez, arXiv:hep-ph/0604112; J. Foster, K. i. Okumura and L. Roszkowski, arXiv:hep-ph/0604121; P. Ball and R. Fleischer, arXiv:hep-ph/0604249.
[7] <http://www-d0.fnal.gov/Run2Physics/WWW/results/prelim/B/B29/B29.pdf>
[8] Y. Grossman, Y. Nir and G. Raz, arXiv:hep-ph/0605028.
[9] Y. Grossman, Phys. Lett. B **380**, 99 (1996); I. Dunietz, R. Fleischer and U. Nierste, Phys. Rev. D **63**, 114015 (2001).
[10] M. Ciuchini *et al.*, JHEP **0107**, 013 (2001); M. Bona *et al.* [UTfit Collaboration], JHEP **0507**, 028 (2005).
[11] M. Bona *et al.* [UTfit Collaboration], JHEP **0603**, 080 (2006).
[12] <http://www.utfit.org>, Summer 2006 update.
[13] J. M. Soares and L. Wolfenstein, Phys. Rev. D **47**, 1021 (1993); N. G. Deshpande, B. Dutta and S. Oh, Phys. Rev. Lett. **77**, 4499 (1996); J. P. Silva and L. Wolfenstein, Phys. Rev. D **55**, 5331 (1997); A. G. Cohen, D. B. Kaplan, F. Lepeintre and A. E. Nelson, Phys. Rev. Lett. **78**, 2300 (1997); Y. Grossman, Y. Nir and M. P. Worah, Phys. Lett. B **407**, 307 (1997).
[14] M. Ciuchini *et al.*, eConf **C0304052**, WG306 (2003) [arXiv:hep-ph/0307195]; S. Laplace, Z. Ligeti, Y. Nir and G. Perez, Phys. Rev. D **65**, 094040 (2002); Z. Ligeti, Int. J. Mod. Phys. A **20**, 5105 (2005); F. J. Botella, G. C. Branco, M. Nebot and M. N. Rebelo, Nucl. Phys. B **725**, 155 (2005); L. Silvestrini, Int. J. Mod. Phys. A **21**, 1738 (2006); K. Agashe, M. Papucci, G. Perez and D. Pirjol, arXiv:hep-ph/0509117.
[15] M. Acciarri *et al.* [L3 Collaboration], Phys. Lett. B **438**, 417 (1998); P. Abreu *et al.* [DELPHI Collaboration], Eur. Phys. J. C **16**, 555 (2000); R. Barate *et al.* [ALEPH Collaboration], Phys. Lett. B **486**, 286 (2000); F. Abe *et al.* [CDF Collaboration], Phys. Rev. D **57**, 5382 (1998); D. Acosta *et al.* [CDF Collaboration], Phys. Rev. Lett. **94**, 101803 (2005); <http://www-cdf.fnal.gov/physics/new/bottom/060126.blessed-BsKK>.
<http://www-d0.fnal.gov/Run2Physics/WWW/results/prelim/B/B36/B36.pdf>.

- [16] B. Aubert *et al.* [BABAR Collaboration], Phys. Rev. Lett. **96**, 251802 (2006).
- [17] J. Abdallah *et al.* [DELPHI Collaboration], Eur. Phys. J. C **28**, 155 (2003); B. Aubert *et al.* [BABAR Collaboration], Phys. Rev. Lett. **92**, 181801 (2004).
- [18] S. Eidelman *et al.* [Particle Data Group], Phys. Lett. B **592**, 1 (2004).
- [19] M. Ciuchini *et al.*, JHEP **0308**, 031 (2003).